International Journal of Solids and Structures 47 (2010) 3141–3149

Contents lists available at ScienceDirect

International Journal of Solids and Structures

journal homepage: www.elsevier.com/locate/ijsolstr

Chemo-electro-mechanical modeling of ionic-strength-sensitive hydrogel: Influence of Young's modulus

Fukun Lai, Hua Li *, Rongmo Luo

School of Mechanical and Aerospace Engineering, Nanyang Technological University, 50 Nanyang Avenue, Singapore 639798, Singapore

ARTICLE INFO

Article history:
Received 13 July 2009
Received in revised form 1 July 2010
Available online 3 August 2010

Keywords:
Chemo-electro-mechanical model
Ionic-strength-sensitive hydrogel
Young's modulus

ABSTRACT

In this paper, a chemo-electro-mechanical model is presented which considers the characteristics of the three phases of the ionic-strength-sensitive hydrogel, including the solid polymeric network matrix, interstitial fluid and ionic species. It is termed the multi-effect-coupling ionic-strength-stimulus (MECis) model and composed of Poisson–Nernst–Planck system for diffusion of the chemical ionic species in the interior hydrogel and external solution, associated with the fixed charge equation for simulating the interaction between the fixed charges and mobile ions, and the mechanical equilibrium equation to characterize the deformation behavior of the solid polymeric network matrix. The simulation results of the MECis model are examined by comparing with the experimental data published in open literature. It is demonstrated that the present MECis model could simulate well the responsive behavior of the ionic-strength-sensitive hydrogel quantitatively. The parameter study is conducted by the MECis model for analysis of the influence of the Young's modulus on the characteristics of the smart hydrogel, and it is concluded that the present model can be employed as a good platform for design and optimization of the smart hydrogel-based BioMEMS.

1. Introduction

One of the smart hydrogels is known as the ionic-strength-sensitive hydrogel, if it could respond to the stimulus of the ionic strength of the surrounding solution. Usually it is defined as a three-dimensional network of crosslinked macromolecules with interstitial fluid containing ionic species. The ionic-strength-sensitive hydrogel is often synthesized by compositions of ionizable monomers or polymers, such as itaconic acid (Caykara and Dogmus, 2005) and methacrylamidopropyl trimethylammonium chloride (MAPTAC) (Baker et al., 1992). The hydrogel can absorb a significant amount of biological fluid while maintaining its structure integrity or degrading. Further, the high compatibility and degradable properties of the hydrogel make it applicable for widely promising applications, for example, in soft contact lenes (Lim et al., 2002), drug delivery system (Song et al., 2009; Wei et al., 2009) and biosensor/bioactuator (Justin et al., 2009).

In recent years, the hydrogel has received much research attention due to the increasing applications in medical and pharmaceutical industry. However, most of the works were done experimentally, in order to synthesize novel hydrogels (Abd El-Mohdy, 2007; Markland et al., 1999), to test novel methods for preparation. (Huang et al., 2008), or to investigate the properties of the hydrogel (Dhara et al., 1999; Hooper et al., 1990; Zhao and Moore, 2001). Less attention was given on the theoretical model development of the hydrogel, especially for ionic-strength-sensitive hydrogel. Perhaps, the early modeling work of the hydrogel would be attributed to Flory and Huggins via the Flory–Huggin mean-field treatment of gel polymeric network (Flory, 1941; Huggins, 1941). Based on this model, the Flory–Rehner theory was (Flory and Rehner, 1943a,b), in which the swelling of the hydrogel is considered as a result of three contributions, the polymer–solvent mixing, the deformation of network chains and the concentration difference of mobile counterions between the gel and the solution. The above modeling theories brought a lot of studies on the theoretical development of the polymer networks (Okay et al., 1998; Tanaka et al., 1982).

In terms of modeling of the ionic-strength-sensitive hydrogel however, few works were done. For instance, Hooper et al. (1990) demonstrated a model capable of predicting the swelling equilibrium of neutral and ionized polyacrylamide gels in water or aqueous salt solution. Prange et al. (1989) used Donnan theory for analysis of the effect of solution ionic strength and fixed charge density. Baker et al. (1994,1995) presented a simple Flory-type swelling model with Donnan theory concerning the swelling equilibrium of the hydrogel, made comparison between the simulation and experimental results, in which the polyampholyte hydrogel with negative fixed charge was synthesized as the ionic-strength-sensitive hydrogel and corresponding swelling equilibrium was measured as a function of solution ionic strength and fixed charge

* Corresponding author. Tel.: +65 6790 4953; fax: +65 6792 4062/6791 1859.
E-mail address: lihua@ntu.edu.sg (H. Li).

0020-7683/$ - see front matter © 2010 Elsevier Ltd. All rights reserved.
doi:10.1016/j.ijsolstr.2010.07.014

(Baker et al., 1992). Brannon–Peppas and Peppas proposed a model incorporating the ionic strength I for the ionic contribution to the chemical potential as a driving source to expand the hydrogel. (Brannon-Peppas and Peppas, 1991).

Recently, the research effort is put on the mechanical behavior of the hydrogel. Several macroscopic continuum theories were presented, for mechanical deformation of the hydrogel, (Segalman et al., 1992, 1993; Wallmersperger et al., 2004). They applied momentum conservation law for the mechanical deformation of the hydrogel, and incorporated the strength of the hydrogel into the governing equations based on the assumption that the hydrogel is elastic.

In this paper, a chemo-electro-mechanical model is presented for simulation of the swelling/deswelling of the stimulus-responsive hydrogel to the ionic strength change of surrounding solution, termed the multi-effect-coupling ionic-strength-stimulus (MECis) model. It is composed of several governing equations, including Nernst–Planck, Poisson with fixed charge density and mechanical finite deformation equations. The Nernst–Planck equations characterize the diffusion and convection of the ionic species in the solution, hydrogel and the interface between them, in which the driving sources of the diffusion include the gradients of the concentration, activity coefficient and electrical potential. The activity coefficient is associated with the ionic strength of surrounding solution. The electrical potential is governed by the Poisson equation for the distribution of the fixed charges and electrical potential in the hydrogel and solution. The fixed charge equation is derived to reflect the interaction between the mobile ions in the solution and the fixed charges on the polymeric chains of the hydrogel, based on the Langmuir monolayer theory. The ionic strength of surrounding solution as an important parameter is incorporated into the Nernst–Planck and fixed charge equations instead of boundary conditions. The mechanical equilibrium equation is based on the momentum conservation law, where the driving forces include the osmotic pressure resulting from the concentration difference between the interior hydrogel and external solution, and the repulsive force between the fixed charges in the hydrogel.

In order to examine the present MECis model, the simulation is conducted for comparison with the published experiment in open literature. It is then found that the MECis model can predict the swelling/deswelling behavior of the ionic-strength-sensitive hydrogel quantitatively and qualitatively. Simulations are also carried out for parameter study of the influence of the Young's modulus on the swelling/deswelling characteristics of the hydrogel, especially on the distributions of the positive, negative mobile ions, fixed charges, electrical potential, and displacement.

2. Mathematical model development

The ionic-strength-sensitive hydrogel generally consists of three phases, including the polymeric network solid matrix, interstitial fluid, and ionic species which may be the charges fixed to the polymeric chains or the mobile ions in the interstitial fluid. For modeling of the responsive characteristics of the hydrogel subject to the change in the ionic strength of the surrounding solution, the chemical behavior of the mobile ionic species in the interstitial fluid of the hydrogel and external solution is formulated by considering the transport of the ionic species over the interstitial fluid and external solution due to the gradients of the concentration, electrical potential and activity coefficient, and is given by the Nernst–Planck flux as,

$$\mathbf{j}_k = -\mathbf{D}_k\left(\mathrm{grad}(c_k) + c_k\mathrm{grad}(\ln\gamma_k) + \frac{F}{RT}z_k c_k \mathrm{grad}(\psi)\right) + c_k\mathbf{V} \quad (k=1,2,\ldots), \tag{1}$$

where $\mathbf{j}_k, \mathbf{D}_k(\mathrm{m}^2/\mathrm{s}), \gamma_k, z_k$ are the flux, the diffusivity tensor, the chemical activity coefficient and the valence of the kth ionic species, respectively. ψ(V) is the electrical potential, and $\mathbf{V}$ the convective velocity. F(C/mol),R(J/Kmol) and T(K) are the Faraday constant, universal gas constant and environmental temperature. The Nernst–Planck flux $\mathbf{j}_k$ represents the ionic transport in the hydrogel and solution, as well as over the interface between the hydrogel and solution. The diffusion–convection flux $\mathbf{j}_k$ of the kth ionic species results from three contributions, namely the gradient of the concentration c_k, the gradient of electrical potential ψ as a migration flux due to the electrophoresis, and the migration flux due to the chemical activity coefficient γ_k since it has to be considered for a non-ideal solution or mixture.

Based on the law of mass conservation, the Nernst–Planck continuity equations are written as

$$\begin{aligned}&\dot{c}_k + \mathrm{div}(\mathbf{j}_k) + \upsilon_k r \\ &\quad = \dot{c}_k - \mathrm{div}\left[\mathbf{D}_k\left(\mathrm{grad}(c_k) + c_k\mathrm{grad}(\ln\gamma_k) + \frac{Fz_kc_k}{RT}\mathrm{grad}(\psi)\right)\right] \\ &\quad\quad + \upsilon_k r = 0 \quad (k=1,2,\ldots)\end{aligned} \tag{2}$$

where the convective velocity is neglected, the generation/consumption rate of the ionic species k resulting from chemical reaction is expressed by the product of the stoichiometric coefficient υ_k and the reaction rate r. By the well known Debye–Hukel theory Sinko (2006), the chemical activity coefficient γ_k of the kth ionic species is determined by

$$\ln\gamma_k = \begin{cases} -\ln 10 A z_k^2\sqrt{I} & I\in[0,0.02], \\ -\frac{\ln 10 A z_k^2\sqrt{I}}{1+a_kB\sqrt{I}} & I\in(0.02,0.1], \\ -\ln 10\left(\frac{Az_k^2\sqrt{I}}{1+a_kB\sqrt{I}} - CI\right) & I>0.1, \end{cases} \tag{3}$$

in which, A and B are the factors that depend only on the temperature and the dielectric constant of the medium. I is the ionic strength as a measure of the concentration presented in the solution, and is defined as

$$I = \frac{1}{2}\sum_k z_k^2 c_k \quad (k=1,2,\ldots). \tag{4}$$

The Nernst–Planck continuity Eq. (2) characterize the ionic chemical behavior in both the hydrogel and solution for the distributions of the ions presented in the system. It is also observed that the ionic strength of the surrounding solution determines the activity coefficient and then influences the ionic transport over the solution and hydrogel.

The electrical potential ψ in the Nernst–Planck Eq. (2) is described by the following Poisson equation, based on the assumption that the electrical potential travels much faster than the ions in the interior hydrogel and external solution,

$$\nabla^2\psi = -\frac{F}{\varepsilon_0\varepsilon_r}\left(\sum_k z_k c_k + z_f c_f\right), \tag{5}$$

where c_f and z_f are the concentration and valence of the fixed charge in the hydrogel, respectively. ε_0 and ε_r are the vacuum and relative permittivities, respectively. Poisson equation characterizes the interaction between ionic species and electrical potential in both the interior hydrogel and external solution. In the hydrogel region, the electric potential depends on the concentrations of both the mobile ions and fixed charges, while it is dependent on mobile ions only in the surrounding solution.

The Poisson–Nernst–Planck (PNP) system (2) and (5) are formulated only in the deformed configuration with spatial coordinates system $\mathbf{x}$. However, in order to trace the characteristics of the material points of the hydrogel and solution, usually, it is better

to use the material coordinates $\mathbf{X}$ in undeformed configuration. After transformation of the coordinate system, the PNP system (2) and (5) are rewritten as

$$\dot{c}_k = J^{-1}\mathrm{div}_X\left[JD_k\mathbf{C}^{-1}\left(\mathrm{grad}_X c_k + c_k\mathrm{grad}_X \ln\gamma_k + \frac{Fz_kc_k}{RT}\mathrm{grad}_X\psi\right)\right] + \upsilon_k r \quad (k=1,2,\ldots), \tag{6}$$

$$\mathrm{div}_X\left(J\mathbf{C}^{-1}\mathrm{grad}_X\psi\right) = -\frac{JF}{\varepsilon_0\varepsilon_r}\left(\sum_k z_kc_k + z_fc_f\right) \quad (k=1,2,\ldots), \tag{7}$$

where J is Jacobian of the deformation gradient, $\mathbf{C}^{-1}$ is the inverse of the Cauchy–Green strain tensor of the solid polymeric networks of the hydrogel.

Next, let's consider the properties of fixed charges in the hydrogel. As well known, the ionizable groups of the hydrogel would dissociate when immersed into solution. The dissociation reaction leaves the fixed charges on the polymeric chains, and then they would bind mobile ions diffusing from the external solution. This dissociation and binding processes may be characterized by Chen et al. (2003)

$$\begin{aligned} &-\mathrm{COOH} \overset{K_a}{\leftrightarrow} -\mathrm{COO}^- + \mathrm{H}^+ \\ &-\mathrm{COO}^- + \mathrm{Na}^+ \overset{K_b}{\leftrightarrow} -\mathrm{COONa}, \end{aligned} \tag{8}$$

if the ionizable groups is presented in the form of −COOH and a solution with Na^+, where K_a and K_b are dissociation and binding constants, respectively. The interaction between the fixed charges and the mobile ions could be modeled by the Langmuir monolayer theory, which gives the fixed charge density equation as. (Luo et al., 2007)

$$c_f = \frac{1}{1+H}\frac{c_{f,s}^0 K}{K+c_b}, \tag{9}$$

where $c_{f,s}^0$ is the concentration of the total fixed charge groups in the hydrogel at a relaxed state (e.g. initial state without deformation), c_b is the concentration of the mobile ions which may be bound to the fixed charge sites on the polymeric chains of the hydrogel. $H = V^w/V^s$ is the local hydration defined as the ratio of the interstitial fluid volume V^w to the solid polymeric phase volume V^s. $K(\mathrm{mol/m^3})$ denotes the apparent dissociation or binding constant of the hydrogel, and it is expressed by Sinko (2006)

$$K = K_0\exp\left[A\ln(10)(2n-1)\sqrt{I}/(1+\sqrt{I})\right], \tag{10}$$

where K_0 is the intrinsic dissociation or binding constant, n the absolute value of valence of the ionizable fixed charge. Transforming Eq. (9) into the reference configuration leads to

$$c_f = \frac{c_{f,s}^0\phi_0^s K_0\exp\left[A\ln(10)(2n-1)\sqrt{I}/(1+\sqrt{I})\right]}{J\left(K_0\exp\left[A\ln(10)(2n-1)\sqrt{I}/(1+\sqrt{I})\right]+c_b\right)}, \tag{11}$$

where ϕ_0^s is the volume fraction of the solid polymeric phase of the hydrogel in the reference configuration. The interaction between the fixed charges and mobile ions plays an important role in the swelling of the hydrogel, and the ionic strength I influences the dissociation degree significantly.

Finally, let's consider the mechanical characteristic of the solid polymeric networks of the hydrogel. The solid polymeric matrix furnishes the structural and physical integrity of the hydrogel, and guarantees the hydrogel exhibiting a reversibly swelling or shrinking in aqueous medium. This is based on the conversation law of linear momentum. Based on the assumption that the hydrogel is immersed in an unstirred solution without vibration, the mechanical equilibrium governing equation in the reference configuration is

$$\nabla\cdot\mathbf{P} = 0, \tag{12}$$

where $\mathbf{P}$ is the first Piola–Kirchhoff stress tensor, and it results from the three contributions, the nominal osmotic pressure $\mathbf{P}^o$, the nominal elastic stress $\mathbf{P}^e$, and the nominal chemical expansion stress $\mathbf{P}^r$ due to electrostatic repulsive force between the fixed charges, namely

$$\mathbf{P} = \mathbf{P}^o + \mathbf{P}^r + \mathbf{P}^e. \tag{13}$$

The nominal osmotic pressure $\mathbf{P}^o$ in the reference configuration is obtained by transforming from the hydrostatic osmotic pressure $p_{osmotic}$ in the current configuration, which is produced by the difference of ionic concentrations between the interior hydrogel and external solution, and it is calculated by

$$\mathbf{P}^o = -J\mathbf{F}^{-1}p_{osmotic}\mathbf{I} = -J\mathbf{F}^{-1}RT\sum_k(c_k - c_{k0})\mathbf{I}, \tag{14}$$

where c_{k0} and c_k are the concentrations of the kth ion species in buffer solution and the hydrogel, respectively.

The chemical expansion stress $\mathbf{P}^r$ due to the electrostatic repulsive force between the fixed charges within the hydrogel can be formulated by

$$\mathbf{P}^r = -J\mathbf{F}^{-1}\frac{Fc_fq\|\mathbf{R}\|}{4\pi\varepsilon_0\|\mathbf{r}\|}\left(\frac{\|\mathbf{r}\|+\kappa}{\|\mathbf{r}\|\kappa}\right)\exp\left(-\frac{\|\mathbf{r}\|}{\kappa}\right)\mathbf{I}, \tag{15}$$

where the scalar $\|\mathbf{R}\|$ and $\|\mathbf{r}\|$ are the mean distances of the fixed charges in the reference and current configurations respectively, and $\|\mathbf{r}\| = \|\mathbf{F}\|\|\mathbf{R}\|$. In the present MECis model, the mesh size is considered as a mean distance between the fixed charges, which represents the average distance between the consecutive crosslinks and serves as an indicator of the screening effect of the polymeric network on solute diffusion (Canal and Peppas, 1989; Peppas et al., 1985). Eq. (15) is derived according to Debye–Huckel model, in which the electrostatic potential of a point charge q is determined by a basic Eq. (16) that can be found in many textbooks (e.g., (Bellan, 2006))

$$\Phi(\mathbf{r}) = \frac{q}{4\pi\varepsilon_0\|\mathbf{r}\|}\exp\left(-\frac{\|\mathbf{r}\|}{\kappa}\right), \tag{16}$$

where κ is called Debye radius and defined as

$$\kappa = \sqrt{\frac{\varepsilon kT}{2N_Aq^2I_h}}, \tag{17}$$

in which, k, N_A and I_h are Boltzmann constant, Avogadro constant and the ionic strength of the interstitial solution within the hydrogel. Based on the isotropic and homogeneous assumption, the fixed charges are distributed uniformly in the hydrogel. The number of total fixed charges can be calculated by $N = c_fVN_A$. If all the fixed charges have the same potential energy expressed by Eq. (16), the total potential energy $w(r)$ due to the electrostatic repulsive force among all the charges is derived as

$$w(\mathbf{r}) = \frac{Nq^2}{4\pi\varepsilon_0\|\mathbf{r}\|}\exp\left(-\frac{\|\mathbf{r}\|}{\kappa}\right). \tag{18}$$

The density of potential energy is thus given by

$$\varphi(\mathbf{r}) = \frac{w(\|\mathbf{r}\|)}{V} = \frac{Fc_fq}{4\pi\varepsilon_0\|\mathbf{r}\|}\exp\left(-\frac{\|\mathbf{r}\|}{\kappa}\right). \tag{19}$$

Therefore, the nominal repulsion stress is determined by the derivative of repulsive density of potential energy with respect to the deformation gradient, namely

$$\begin{aligned} \mathbf{P}^r &= \frac{\partial\varphi(\mathbf{r})}{\partial\mathbf{F}} = \frac{\partial\varphi(\mathbf{r})}{\partial\|\mathbf{r}\|}\frac{\partial\|\mathbf{r}\|}{\partial J}\frac{\partial J}{\partial\mathbf{F}} = \|\mathbf{R}\|\frac{\partial\varphi(\mathbf{r})}{\partial\|\mathbf{r}\|}J\mathbf{F}^{-T} \\ &= -\frac{Fc_fq\|\mathbf{R}\|}{4\pi\varepsilon_0\|\mathbf{r}\|}\left(\frac{\|\mathbf{r}\|+\kappa}{\|\mathbf{r}\|\kappa}\right)\exp\left(-\frac{\|\mathbf{r}\|}{\kappa}\right)J\mathbf{F}^{-T}. \end{aligned} \tag{20}$$

For simplification, we prescribe

$$p_{repulsion} = \frac{Fc_f q\|\mathbf{R}\|}{4\pi\varepsilon_0\|\mathbf{r}\|}\left(\frac{\|\mathbf{r}\|+\kappa}{\|\mathbf{r}\|\kappa}\right)\exp\left(-\frac{\|\mathbf{r}\|}{\kappa}\right). \tag{21}$$

The nominal repulsion stress is thus rewritten as

$$P^r = -J\mathbf{F}^{-1}p_{repulsion}\mathbf{I}. \tag{22}$$

In addition, the nominal elastic stress $\mathbf{P}^e$ is associated with a constitutive relation and the second Piola–Kirchhoff stress tensor $\mathbf{S}$ as

$$\mathbf{P}^e = \mathbf{S}\mathbf{F}^T, \tag{23}$$

where the second Piola–Kirchhoff stress is given by the constitutive equation of the hydrogel as

$$\mathbf{S} = \mathbf{D}\mathbf{E}, \tag{24}$$

where $\mathbf{D}$ is the material moduli tensor.

As a result, the mechanical equilibrium equation is written as

$$\mathrm{div}\left[\mathbf{S}\mathbf{F}^T - J\mathbf{F}^{-1}(p_{osmotic}+p_{repulsion})\mathbf{I}\right] = 0. \tag{25}$$

Here, it is noted that swelling or shrinking of the ionic-strength-sensitive hydrogel is drived by both the osmotic pressure $p_{osmotic}$ and repulsive force $p_{repulsion}$.

The development of MECis model has so far been completed. It is composed of the coupled nonlinear partial differential governing equations, including Nernst–Planck Eq. (6), Poisson Eq. (7) with the formula of fixed charge density (11) and mechanical Eq. (25), for simulation of the ionic-strength-sensitive hydrogel. The MECis model considers the three phases of the hydrogel and the surrounding solution as well as the chemical, electrical and mechanical multi-energy domains. In the presently developed model, the ionic strength I of bathing solution is considered as a variable coefficient in the partial differential governing equations, instead of boundary conditions, because it is a key stimulus to the swelling/shrinking of the present smart hydrogel, and has the significant influence on the ionic transport between the hydrogel and surrounding solution, and on the fixed charge density in the hydrogel, as well as on the osmotic pressure and the repulsive force.

3. Result and discussion

In the subsequent simulation, the hydrogel disks are investigated for analysis of the equilibrium swelling ratio and other characteristics. The swelling is isotropic within the disk plane without rotation, and therefore the computational domain can be reduced to one-dimension in the radial direction. As such, the one-dimensional form of the MECis model will be applied along the radial direction to analyze the smart hydrogel responsive to the external ionic strength, and to investigate the influence of the different Young's moduli on the equilibrium swelling characteristics. The equilibrium swelling ratio ESR can thus be defined as

$$ESR = \frac{\pi d^2 h/4}{\pi d_0^2 h/4} = \frac{d^2}{d_0^2}, \tag{26}$$

where d and d_0 are the swollen and initial diameter of the hydrogel, respectively, and h is the height of the disk.

3.1. Validation of the MECis model

For examining the present MECis model with the capability of predicting the swelling/deswelling behavior of the ionic-strength-sensitive hydrogel, the simulation results are compared with the experimental data (Dhara et al., 1999), where the poly (AAm-*co*-AA)-PVA (PAAP) hydrogel disk was synthesized by different weight fractions of acrylamide (AAm), acrylic acid (AA) and poly (vinyl alcohol) (PVA) (Dhara et al., 1999). The comparison is made for the A3 series of PAAP hydrogel in this paper. The A3 series of PAAP hydrogel was synthesized by weight fraction of 60% AAm, 15% AA and 25% PVA, and by crosslinking PVA with different time, 0 and 80 min. As a result, two types of the hydrogel were prepared and named T0 and T80. The acrylic acid can dissociate in solution, such that the corresponding concentration can be employed as the fixed charge density and its dissociation constant is found (Burke and Barrett, 2003; Vink, 1986). All the input data for simulation of the PAAP hydrogel are listed in Table 1.

Fig. 1 demonstrates the comparison for the A3 series of PAAP hydrogel between the simulation results by the MECis model and the experimental data (Dhara et al., 1999), where the experimental data are presented by symbols and the simulation results by lines. As observed from the figure, with the increase of the ionic strength of surrounding solution, the ionic-strength-sensitive hydrogel shrinks by following three stages. Firstly, the decrease of swelling will slow down when the ionic strength of the solution increases up to 1 M due to the interaction between the mobile natrium ions and the fixed charge groups on the polymeric chains. In this stage, the binding reaction between the natrium ions and fixed charges is still quite active, such that the increase of the ionic strength of the external solution enlarges the concentration of the ions inside the hydrogel and then the osmotic pressure over the hydrogel-solution interface is altered slightly. As such, the swelling ratio of the hydrogel changes slowly. Secondly, after an optimum of ionic natrium to the polymer chains binding at the ionic strength of

Table 1
The input data of MECis model for the simulation of A3 series of PAAP hydrogel.

Parameters	*Values* (for both T0 and T80)
Environmental ionic strength I(M) (Dhara et al., 1999)	$10^{-4} \sim 3$
Initial diameter of hydrogel (mm) (Dhara et al., 1999)	18
Initial fixed charge density (mM)	2.6006
Initial mesh size r_0 (nm) (Shukla and Bajpai, 2006)	$8.2 \sim 73.1$
Intrinsic dissociation constant pK_0 (M) (Burke and Barrett, 2003; Kortum et al., 1961; Vink, 1986)	3.6
Temperature T (K) (Dhara et al., 1999)	298
The factor of activity coefficient A (Sinko, 2006)	0.51
Valence of fixed charge z_f (Dhara et al., 1999)	−1
Parameters	*Values*
Young's modulus E_Y (MPa) (Lopez-Ureta et al., 2008; Martens et al., 2007)	0.18 (T0), 0.6 (T80)

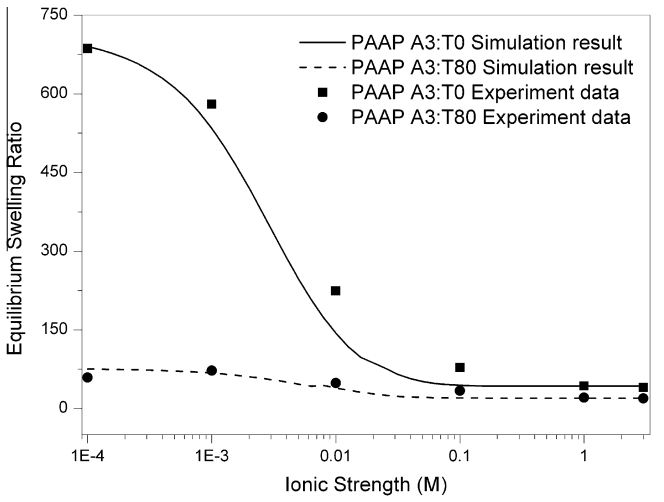

Fig. 1. Comparison for A3 series of PAAP hydrogel between the simulation results of MECis model and experimental data (Dhara et al., 1999).

about 1 mM, further increase of the ionic strength reduces the concentration gap significantly over the interface between hydrogel and solution which leads to the reduction of the osmotic pressure and repulsive force (Caykara and Dogmus, 2005). Thus the hydrogel shrink drastically when the ionic strength ranges between 1 mM and 100 mM. In the third stage, the swelling ratio varies insignificantly when the ionic strength is larger than 100 mM. The possible reason is that, after the significant shrinking of the hydrogel in the second stage, at the ionic strength of about 100 mM, the hydrogel stays in compact state already, further increase of the ionic strength may not change the compacted state of the hydrogel any more (Caykara and Dogmus, 2005). In addition, it is also noted that the low ionic strength leads to the large Debye length that strengthens the repulsive force, while the high ionic strength decreases the Debye length that declines the effect of repulsive force on the swelling of the hydrogel. The shrinking phenomenon was also studied by the Flory-type mean-field theory (Tanaka, 1979; Tanaka et al., 1980).

It could also be observed from Fig. 1 that the MECis model predicts well the mechanical property of the hydrogel and its effect on the swelling behavior. As well known, the crosslinking time affects the strength of the hydrogel and thus the Young's modulus varies by different crosslinking time (Schroder and Oppermann, 1996). For the A3 series of PAAP hydrogel, the T0 type of Young's modulus is smaller than the T80 type of that, because of the different crosslinking time. The experiments also show clearly that the swelling ratio of PAAP hydrogel decreases with the increase of the crosslinking time, when the hydrogel is immersed in the solution with the same ionic strength. The simulation results fit the experimental data quite well for different Young's moduli of the hydrogel.

By the above comparison between the simulation and the experiment, it is concluded that the MECis model can simulate well the responding deformation of the hydrogel to the stimulus of ionic strength of surrounding solution, and can be employed as a good tool for analysis of the influence of the Young's modulus on the characteristics of the ionic-strength-sensitive hydrogel.

3.2. Parameter study

As the most important mechanical property of material, Young's modulus is used widely for evaluation of the strength of the hydrogel assumed as an elastic and isotropic mixture. In general, the Young's modulus of the hydrogel could be modified by changing the crosslinking time, using monomers with large modulus, or altering amount of total monomer during synthesis (David et al., 2004; Martens et al., 2007; Matzelle et al., 2003; Srivastava et al., 2007). The elastic modulus of some hydrogels may also change with the environmental conditions, such as temperature and concentration of surrounding solution (Wang et al., 1997; Ye et al., 2004). In the past, the studies on the effect of Young's modulus on the swelling ratio were experiment-based (Baker et al., 1994; Dhara et al., 1999; Hooper et al., 1990). Few of them were involved in theoretical modeling (De et al., 2002; Hong et al., 2010; Wallmersperger and Kroplin, 2007; Zhao et al., 2008). In this section, the MECis model validated will be employed for discussion of Young's modulus of the hydrogel especially focusing on the effect of the variation of Young's modulus on the concentration distribution of concentration natrium and chlorine ions, fixed charge density, electric potential, displacement and swelling ratio. The input data used in the parameter study are given as, the valence of the fixed charge $z_f = -1$, the initial length of gel domain $LGel0 = 4$ mm, environmental temperature $T = 298$ K, the length of solution domain $L = 10$ mm, initial mesh size $r_0 = 600$ Å, intrinsic dissociation constant $pK_0 = 3.6$, and the initial fixed charge density $c^0_{f,s} = 800$ mM.

The dependence of normalized swelling ratio on Young's modulus is shown in Fig. 2. As it is observed from the figure, the

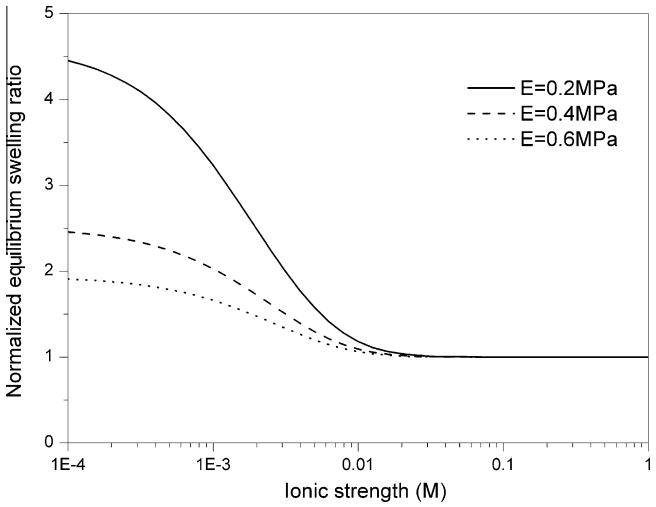

Fig. 2. Influence of Young's modulus on the swelling behavior of the ionic-strength-sensitive hydrogel for various environmental ionic strengths.

Young's modulus influences significantly the equilibrium swelling ratio of the ionic-strength-sensitive hydrogel when immersed in the solution with low ionic strength, e.g. less than 10 mM. However, the change of Young's modulus has insignificant effects on the equilibrium swelling ratio of the hydrogel placed in a solution with high ionic strength, e.g. larger than 10 mM. This interesting observation may result from the different states of the hydrogel when immersed in solution with different ionic strengths. For example, if the environmental solution has low ionic strength, the hydrogel swells greatly due to the binding reaction between the mobile ions and the fixed charge sites, and the increase of the Young's modulus may enhance the stiffness of the hydrogel, which reduces the deformation flexibility of the hydrogel (Sasaki, 2006; Schroder and Oppermann, 1996; Srivastava et al., 2007). As a result, the swelling ratio drops with the increase of the Young's modulus of the hydrogel at a low ionic strength of surrounding solution. However, when the solution has high ionic strength, the hydrogel doesn't swell or swells trivially, and the Young's modulus changes the state of the hydrogel insignificantly.

It is also seen from Fig. 2 that the equilibrium swelling ratio decreases with the increase of Young's modulus, and the interval between adjacent curves also decreases. This performance is observed from Fig. 3 more significantly, in which it decreases fast initially until Young's modulus of about 0.6 MPa, and then becomes slow. Fig. 3 also shows the different characteristics of the ionic-strength-sensitive hydrogel in the solution with low and high ionic strengths respectively, where the Young's modulus influences the swelling ratio of ionic-strength-sensitive hydrogel exponentially nonlinearly for low ionic strength and almost linearly for high ionic strength, respectively.

Figs. 4 and 5 exemplify the distributive profile of the fixed charge density within the hydrogel as a function of Young's modulus, when the ionic strengths of bath solution are 1 mM and 100 mM, respectively. As observed from Fig. 4, increasing Young's modulus leads to a smaller swelling, and thus to a smaller decrease of the concentration of fixed charges. The binding reaction between the fixed charge density and mobile ions is mainly influenced by the deformation of the hydrogel, if Young's modulus is changed. Therefore, the variation of the fixed charge density is almost controlled by the deformation of the hydrogel. From mathematical point of view, the fixed charge density is the function of the initial fixed charge density $c^s_{f,0}$, the ionic strength I, the concentration of binding ions c_b, the intrinsic dissociation or binding constant K_0, and the Jacobian of the hydrogel J, as described in Eq. (11).

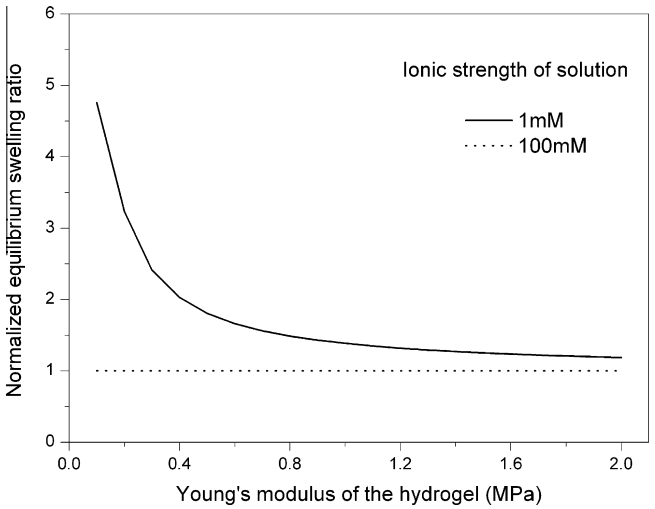

Fig. 3. Influence of Young's modulus on the swelling behavior of the ionic-strength-sensitive hydrogel immersed in the solution with the ionic strength of 1 mM and 100 mM.

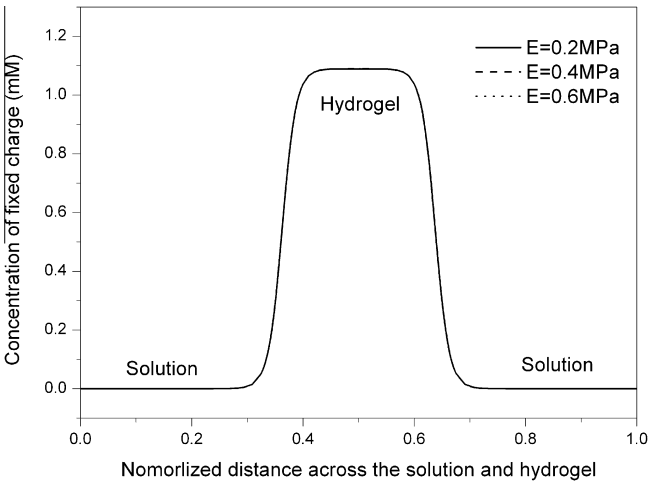

Fig. 5. Influence of Young's modulus on the fixed charges density c_f of the hydrogel if the ionic strength of external solution is 100 mM.

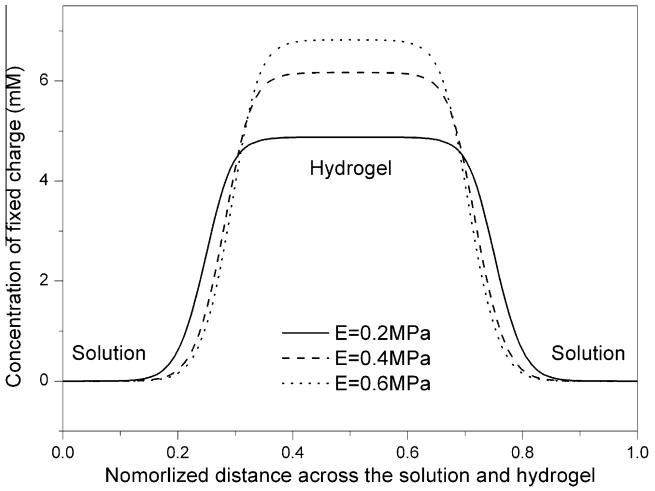

Fig. 4. Influence of Young's modulus on the fixed charges density c_f of the hydrogel if the ionic strength of external solution is 1 mM.

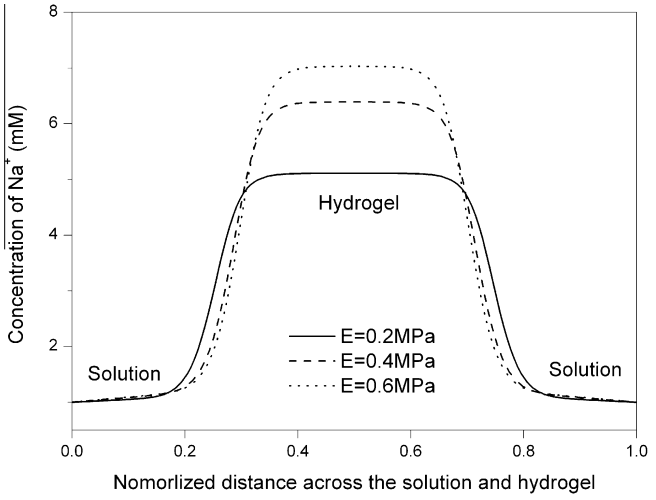

Fig. 6. Influence of Young's modulus on the distribution of sodium ion concentration c_{Na^+} if the ionic strength of external solution is 1 mM.

If $c^s_{f,0}$, I, K_0 and c_b are given, the Jacobian of the hydrogel J is the only what can influence the fixed charge density. As Young's modulus increases, the hydrogel shrinks and then the Jacobian J decreases, the fixed charge density thus increases. However, the influence of the Young's modulus on the fixed charge density is quite insignificant when the hydrogel is placed into a solution with the ionic strength of 100 mM, as observed from Fig. 5. This may result from the deformation of the hydrogel. At the ionic strength of 100 mM, the hydrogel almost remains a compact state, and the variation of the swelling is insignificant with Young's modulus. The fixed charge density thus changes slightly. In fact, there exists a jump of the fixed charge density over the hydrogel-solution interface, as formulated in Eq. (11), which is defined in the hydrogel domain only for the fixed charge density. In other words, theoretically the MECis model has handled the jump of c_f over the hydrogel-solution interface. In the numerical simulation however, the exact discontinuous field is difficultly achieved. The gradual change of the fixed charge density over the hydrogel-solution, as shown in Fig. 4, results from the computational approximation. This will be improved in the future.

The distributive pattern of natrium ion concentration c_{Na^+} is almost similar to that of the fixed charge density, as observed from Fig. 6. The fixed charges with the valence of -1 attract the natrium ions into and repel the chlorine ions out of the hydrogel to maintain the electroneutrality inside the hydrogel. Therefore, the concentration of the natrium ions c_{Na^+} increases with the fixed charge density in the interior hydrogel, and keeps constant in the external solution. By contrast, the concentration of the chlorine ions c_{Cl^-} decreases with the increase of the Young's modulus as known from Fig. 8 for the ionic strength of 1 mM. However, the distributions of the natrium and chlorine ions in the solution with the ionic strength of 100 mM also change slightly, as observed from Figs. 7 and 9. It is also noted in Figs. 6 and 8 that the electroneutrality condition in the solution domain is not satisfied exactly. This results from the computational error accumulation during the iteration process for convergence, due to the large difference between the initial fixed charge density and the ionic strength.

The profiles of the electrical potential distributed in the hydrogel and solution are illustrated in Figs. 10 and 11. The electrical potential is associated with the concentration of mobile ions and/or fixed charges, as shown in Eqs. (5) and (7). In the environmental solution, the electrical potential remains constant since the electroneutrality condition is already satisfied. In the hydrogel, however, there is a small difference between the concentrations of

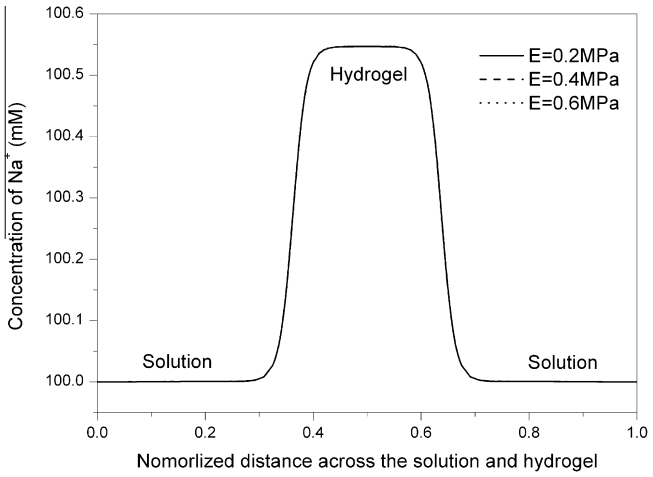

Fig. 7. Influence of Young's modulus on the distribution of sodium ion concentration c_{Na^+} if the ionic strength of external solution is 100 mM.

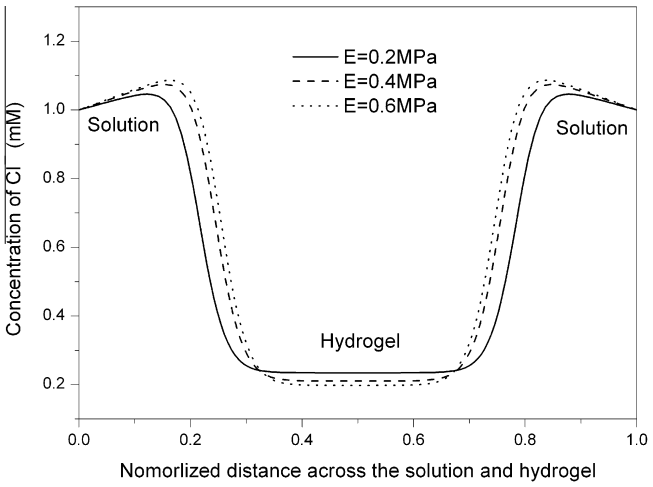

Fig. 8. Influence of Young's modulus on the distribution of chlorines ion concentration c_{Cl^-} if the ionic strength of external solution is 1 mM.

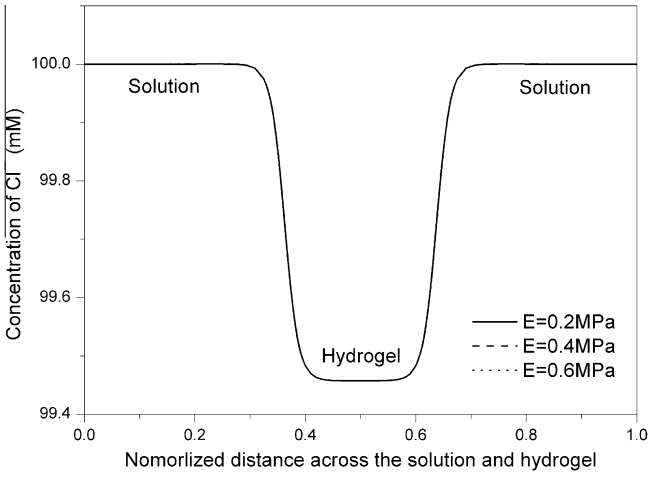

Fig. 9. Influence of Young's modulus on the distribution of chlorine ion concentration c_{Cl^-} if the ionic strength of external solution is 100 mM.

positive and negative ions, which produces the nonzero electrical potential. With the increase of Young's modulus, the difference increases and thus it enlarges the electrical potential.

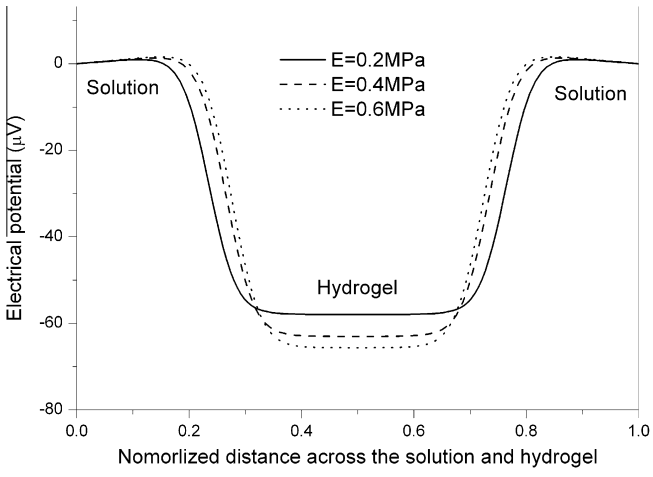

Fig. 10. Influence of Young's modulus on the distribution of electrical potential ψ if the ionic strength of external solution is 1 mM.

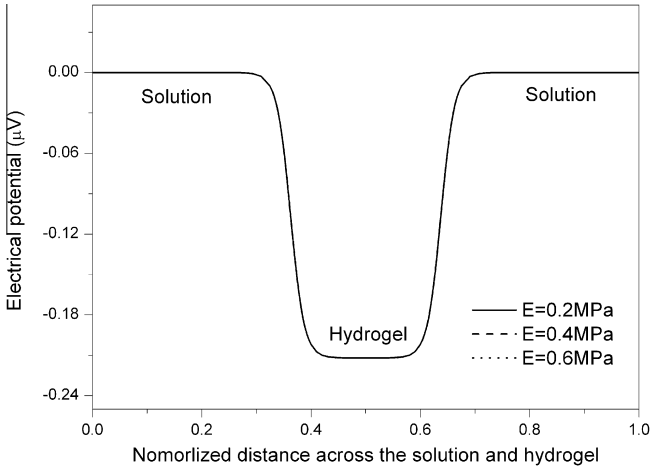

Fig. 11. Influence of Young's modulus on the distribution of electrical potential ψ if the ionic strength of external solution is 100 mM.

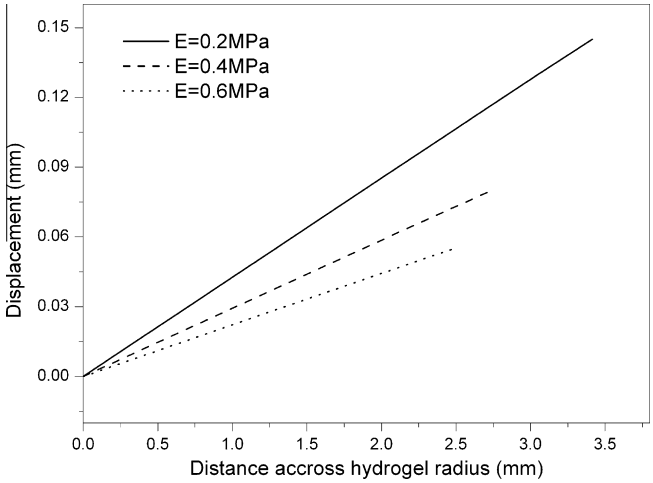

Fig. 12. Influence of Young's modulus on the displacement u of the hydrogel if the ionic strength of external solution is 1 mM.

The displacement profiles of hydrogel are illustrated in Figs. 12 and 13, where only half domain of the displacement field of the hydrogel is necessarily shown since the deformation is symmetric.

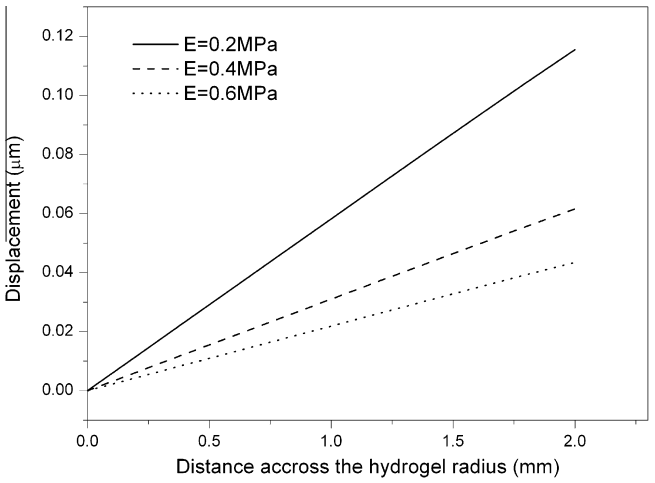

Fig. 13. Influence of Young's modulus on the displacement u of the hydrogel if the ionic strength of external solution is 100 mM.

The effect of Young's modulus on the displacement seems to be quiet directly due to the apparent relation between the displacement and Young's modulus in the mechanical equilibrium Eq. (25). The displacement of the hydrogel is changed largely with the variation of Young's modulus when the hydrogel is immersed into lower ionic strength solution. The large Young's modulus strengthens the hydrogel and makes the polymeric network be more compact. Since the osmotic pressure and repulsive force as driving source are equilibrated by the network strength, increasing Young's modulus could equilibrate larger driving force. As such, the strain of the hydrogels becomes smaller with increasing Young's modulus, which obviously leads to the small displacement.

4. Conclusion

The chemo-electro-mechanical MECis model has been presented for analysis of the influence of Young's modulus on the characteristics of the ionic-strength-sensitive hydrogel. The model considers the three phases of the smart hydrogel including the solid polymeric network matrix, interstitial fluid and ionic species and their response to the ionic-strength-stimulus. The model consists of the governing equations, including Poisson–Nernst–Planck system associated with the fixed charge equation for the ionic species and interstitial fluid, and the mechanical equation for the equilibrium of polymeric network of the hydrogel. The simulation results by the MECis model are compared with the experimental work, and it demonstrates that the MECis model is able to predict the responsive characteristics of ionic-strength-sensitive hydrogel quite well. The parameter studies for the influence of the Young's modulus are conducted on the performance of the ionic-strength-stimulus-responsive hydrogel. It is showed that the Young's modulus has significant effect on the distribution of the mobile ions, fixed charges, electrical potential, displacement and swelling ratio of the smart hydrogel. The comparison and parameter study also conclude that the present MECis model can work as a good platform for design and optimization of smart hydrogel-based BioMEMS.

References

Abd El-Mohdy, H.L., 2007. Water sorption behavior of CMC/PAM hydrogels prepared by [gamma]-irradiation and release of potassium nitrate as agrochemical. React. Funct. Polym. 67, 1094–1102.

Baker, J.P., Blanch, H.W., Prausnitz, J.M., 1995. Swelling properties of acrylamide-based ampholytic hydrogels: comparison of experiment with theory. Poly 36, 1061–1069.

Baker, J.P., Hong, L.H., Blanch, H.W., Prausnitz, J.M., 1994. Effect of initial total monomer concentration on the swelling behavior of cationic acrylamide-based hydrogels. Macromolecules 27, 1446–1454.

Baker, J.P., Stephens, D.R., Blanch, H.W., Prausnitz, J.M., 1992. Swelling equilibria for acrylamide-based polyampholyte hydrogels. Macromolecules 25, 1955–1958.

Bellan, P.M., 2006. Fundamentals of Plasma Physics. Cambridge University Press, Cambridge.

Brannon-Peppas, L., Peppas, N.A., 1991. Equilibrium swelling behavior of pH-sensitive hydrogels. Chem. Eng. Sci. 46, 715–722.

Burke, S.E., Barrett, C.J., 2003. Acid–base equilibria of weak polyelectrolytes in multilayer thin films. Langmuir 19, 3297–3303.

Canal, T., Peppas, N.A., 1989. Correlation between mesh size and equilibrium degree of swelling of polymeric networks. J. Biomed. Mater. Res. 23, 1183–1193.

Caykara, T., Dogmus, M., 2005. Swelling–shrinking behavior of poly(acrylamide-co-itaconic acid) hydrogels in water and aqueous NaCl solutions. J. Macromol. Sci., Part A: Pure Appl. Chem. 42, 105–111.

Chen, Y.M., Matsumoto, S., Gong, J.P., Osada, Y., 2003. Effect of hydrophobic side chain on poly(carboxyl acid) dissociation and surfactant binding. Macromolecules 36, 8830–8835.

David, C.L., Bernard, Y., Noshir, A.L., 2004. Mechanical properties of a reversible, DNA-crosslinked polyacrylamide hydrogel. J. Biomech. Eng. 126, 104–110.

De, S.K., Aluru, N.R., Johnson, B., Crone, W.C., Beebe, D.J., Moore, J., 2002. Equilibrium swelling and kinetics of pH-responsive hydrogels: models, experiments, and simulations. J. Microelectromech. Syst. 11, 544–555.

Dhara, D., Nisha, C.K., Chatterji, P.R., 1999. Super absorbent hydrogels: interpenetrating networks of poly(acrylamide-co-acrylic acid) and (poly vinyl alcohol): swelling behavior and structureal parameters. J. Macromol. Sci., Part A: Pure Appl. Chem. 36, 197–210.

Flory, J.P., 1941. Thermodynamics of high polymer solutions. J. Chem. Phys. 9, 660.

Flory, P.J., Rehner, J.J., 1943a. Statistical mechanics of cross-linked polymer networks I. rubberlike elasticity. J. Chem. Phys. 11, 512–520.

Flory, P.J., Rehner, J.J., 1943b. Statistical mechanics of cross-linked polymer networks II. swelling. J. Chem. Phys. 11, 521–526.

Hong, W., Xuanhe, Z., Zhigang, S., 2010. Large deformation and electrochemistry of polyelectrolyte gels. J. Mech. Phys. Solids 58, 558–577.

Hooper, H.H., Baker, J.P., Blanch, H.W., Prausnitz, J.M., 1990. Swelling equilibria for positively ionized polyacrylamide hydrogels. Macromolecules 23, 1096–1104.

Huang, J., Hu, X., Zhang, W., Zhang, Y., Li, G., 2008. pH and ionic strength-responsive photonic polymers fabricated by using colloidal crystal templating. Colloid. Polym. Sci. 286, 113–118.

Huggins, M.L., 1941. Solutions of long chain compounds. J. Chem. Phys. 9, 440.

Justin, G., Finley, S., Abdur Rahman, A., Guiseppi-Elie, A., 2009. Biomimetic hydrogels for biosensor implant biocompatibility: electrochemical characterization using micro-disc electrode arrays (MDEAs). BioMi.

Kortum, G., Vogel, W., Andrussow, K., 1961. Dissociation Constants of Organic Acids in Aqueous Solution. Butter Worths, London.

Lim, L., Loughnan, M.S., Sullivan, L.J., 2002. Microbial keratitis associated with extended wear of silicone hydrogel contact lenses. Br. J. Ophthalmol. 86, 355–357.

Lopez-Ureta, L.C., Orozco-Guareno, E., Cruz-Barba, L.E., Gonzalez-Alvarez, A., Bautista-Rico, F., 2008. Synthesis and characterization of acrylamide/acrylic acid hydrogels crosslinked using a novel diacrylate of glycerol to produce multistructured materials. J. Polym. Sci., Part A: Polym. Chem. 46, 2667–2679.

Luo, R., Li, H., Lam, K., 2007. Modeling and simulation of chemo-electro-mechanical behavior of pH-electric-sensitive hydrogel. Anal. Bioanal. Chem. 389, 863–873.

Markland, P., Zhang, Y., Amidon, G.L., Yang, V.C., 1999. A pH- and ionic strength-responsive polypeptide hydrogel: synthesis, characterization, and preliminary protein release studies. J. Biomed. Mater. Res. 47, 595–602.

Martens, P., Blundo, J., Nilasaroya, A., Odell, R.A., Cooper-White, J., Poole-Warren, L.A., 2007. Effect of poly(vinyl alcohol) macromer chemistry and chain interactions on hydrogel mechanical properties. Chem. Mater. 19, 2641–2648.

Matzelle, T.R., Geuskens, G., Kruse, N., 2003. Elastic properties of poly(N-isopropylacrylamide) and Poly(acrylamide) hydrogels studied by scanning force microscopy. Macromolecules 36, 2926–2931.

Okay, O., Sariisik, S.B., Zor, S.D., 1998. Swelling behavior of anionic acrylamide-based hydrogels in aqueous salt solutions: comparison of experiment with theory. J. Appl. Polym. Sci. 70, 567–575.

Peppas, N.A., Moynihan, H.J., Lucht, L.M., 1985. The structure of highly crosslinked poly(Zhydroxyethy1 methacrylate) hydrogels. J. Biomed. Mater. Res. 19, 397–411.

Prange, M.M., Hooper, H.H., Prausnitz, J.M., 1989. Thermodynamics of aqueous systems containing hydrophilic polymers or gels. AIChE 35, 803–813.

Sasaki, S., 2006. Elastic properties of swollen polyelectrolyte gels in aqueous salt solutions. J. Chem. Phys. 124, 094903–094908.

Schroder, U.P., Oppermann, W., 1996. Properties of polyelectrolyte gels. In: Addad, J.P.C. (Ed.), Physical Properties of Polymeric Gels. John Wiley & Sons, New York.

Segalman, D.J., Witkowski, W.R., Adolf, D.B., Shahinpoor, M., 1992. Theory and application of electrically controlled polymeric gels. Smart. Mater. Struct. 1, 95.

Segalman, D.J., Witkowski, W.R., Rao, R.R., Adolf, D.B., Shahinpoor, M., 1993. Finite element simulation of the 2D collapse of a polyelectrolyte gel disk, in: Vijay, K.V. (Ed.). SPIE, pp. 14–21.

Shukla, S., Bajpai, A.K., 2006. Preparation and characterization of highly swelling smart grafted polymer networks of poly(vinyl alcohol) and poly(acrylic acid-co-acrylamide). J. Appl. Polym. Sci. 102, 84–95.

Sinko, P.J., 2006. Martin's Physical Pharmacy and Pharmaceutical Sciences. Lippincott Williams & Wilkins, PA.

Song, F., Zhang, L.-M., Yang, C., Yan, L., 2009. Genipin-crosslinked casein hydrogels for controlled drug delivery. Int. J. Pharm. 373, 41–47.
Srivastava, A., Jain, E., Kumar, A., 2007. The physical characterization of supermacroporous poly(N-isopropylacrylamide) cryogel: mechanical strength and swelling/de-swelling kinetics. Mater. Sci. Eng.: A 464, 93–100.
Tanaka, T., 1979. Phase transitions in gels and a single polymer. Poly 20, 1404–1412.
Tanaka, T., Fillmore, D., Sun, S.-T., Nishio, I., Swislow, G., Shah, A., 1980. Phase transitions in ionic gels. Phys. Rev. Lett. 45, 1636–1639.
Tanaka, T., Nishio, I., Sun, S.-T., Ueno-Nishio, S., 1982. Collapse of gels in an electric field. Science 218, 467–469.
Vink, H., 1986. Acid–base equilibria in polyelectrolyte systems. J. Chem. Soc., Faraday Trans. 82, 2353–2365.
Wallmersperger, T., Kroplin, B., Gulch, R.W., 2004. Coupled chemo-electro-mechanical formulation for ionic polymer gels-numerical and experimental investigations. Mech. Mater. 36, 411–420.
Wallmersperger, T., Kroplin, D.B.B., 2007. On the modeling of polyelectrolyte gels. Macromol. Symp. 254, 306–313.
Wang, Q., He, L., Huang, J., 1997. Supermolecular structure and mechanical properties of P(AN-AM-AA)/PVA intermacromolecular complex formed through hydrogen bonding. J. Appl. Polym. Sci. 64, 2089–2096.
Wei, L., Cai, C., Lin, J., Chen, T., 2009. Dual-drug delivery system based on hydrogel/micelle composites. Biomaterials 30, 2606–2613.
Ye, L., Huang, R., Wu, J., Hoffmann, H., 2004. Synthesis and rheological behavior of poly[acrylamide-acrylic acid-N-(4-butyl)phenylacrylamide] hydrophobically modified polyelectrolytes. Colloid. Polym. Sci. 282, 305–313.
Zhao, B., Moore, J.S., 2001. Fast pH- and ionic strength-responsive hydrogels in microchannels. Langmuir 17, 4758–4763.
Zhao, X., Hong, W., Suo, Z., 2008. Stretching and polarizing a dielectric gel immersed in a solvent. Int. J. Solid. Struct. 45, 4021–4031.